

# Comparison of the PROCESS systems code with the SONIC divertor code

J. Morris<sup>1</sup>, N. Asakura<sup>2</sup>, Y. Homma<sup>2</sup>, K. Hoshino<sup>3</sup>, M. Kovari<sup>1</sup>

<sup>1</sup>Culham Centre for Fusion Energy, Abingdon, OX14 3DB, UK

<sup>2</sup>National Institutes for Quantum and Radiological Science and Technology (QST), Rokkasho, Aomori 039-3212, Japan

<sup>3</sup>Graduate School of Science and Technology, Keio University, Japan

In a demonstration (DEMO) reactor, mitigation of the large heat load on the divertor target to below material and engineering limits is a key requirement for operation. Systems modelling is used to design entire fusion power plants and therefore has to be able to appropriately capture the divertor challenge. Therefore, it is important to validate these models against comprehensive SOL-divertor simulation codes and experiments. A one dimensional divertor model in PROCESS was investigated, compared to results of 2-D SONIC simulation under the detachment condition. The comparison shows how the 1-D divertor model handles the power loss mechanisms from the outboard mid-plane to the outer divertor target for a DEMO-like condition. Results show good agreement on the calculated value of the total power crossing the separatrix ( $< 5\%$  difference) and the total impurity radiation power  $P_{imp}$  ( $< 10\%$  difference). However, the 1-D profiles show differences in density and temperature at the upstream of the target ( $< 10\text{m}$  of connection length to target, corresponding to several  $10\text{cm}$  in the poloidal length). One reason for this difference is that the 2-D model calculates impurity transport, which produces a variable impurity fraction along the connection length in the divertor, while the 1-D model uses a single averaged value. The SONIC code also considers physical processes not covered in the 1-D model, such as radial transport in the SOL and divertor region. A scan of  $P_{sep}$  values in PROCESS for a DEMO-sized machine show that above  $P_{sep} = 200\text{ MW}$  there is a stronger impact on cost and machine size for higher  $P_{sep}$ .

Keywords: Nuclear Fusion; Systems Codes; DEMO; Divertor; SOL; PROCESS; SONIC

## 1 Introduction

In a nuclear fusion demonstration (DEMO) power plant reduction of the large heat load on the divertor target is a key criterion for a viable and consistent design. The power exhaust in the divertor impacts both the operational performance of the machine and the lifetime of the divertor components.

Systems codes form an integral part of the EUROfusion DEMO research programme [1]. The goals of the EUROfusion DEMO programme are for a reactor that achieves electrical power output (hundreds of  $\text{MW}_e$ ) for long pulse duration ( $> 2\text{ hrs}$ ) [2], while also demonstrating the technology required for a commercial power station. Reduction of the heat load at the divertor target appropriate for the engineering criterion, such as less than  $10\text{ MW/m}^2$ , is a key requirement.

Systems codes are used to analyse large parameter spaces for optimising design solutions that are self-consistent. The models in systems codes are often 0-D and 1-D simplified calculations with the aim of capturing the physics and engineering processes while being computationally fast. Systems modelling is used to design entire fusion power plants and therefore has to be able to provide the divertor heat load and its trade-offs with the other plant systems.

The systems code used for the work reported on here is the UKAEA systems code PROCESS [3, 4]. This work details a comparison of a 1-D SOL and divertor model in PROCESS with the 2-D divertor simulation code SONIC [5, 6]. The comparison shows how the systems code 1-D divertor model handles the power loss mechanisms from the outboard mid-plane to the outer divertor target for a Japanese DEMO (JA-DEMO) example design [6, 7]. The goal of a divertor model in a systems code is to enforce engineering limits, to determine detachment conditions

and to calculate the heat load.

In this paper, we describe the two SOL/divertor models used for the comparison as well as the JA-DEMO input parameters in Section 2, the results from the comparison are outlined in Section 3 and the work is summarised in Section 4.

## 2 PROCESS Divertor Model and SONIC Code

For reactor design work a number of key divertor protection parameters have been used to try and account for the allowable power going to the target. One commonly used divertor power handling parameter is given below [8, 9].

$$P_{sep}/R_0 < p_{ref} \text{ MWm}^{-1} \quad (1)$$

where  $P_{sep}$  is the power conducted across the plasma separatrix (MW),  $R_0$  is the plasma major radius (m) and  $p_{ref}$  is determined by the power exhaust concepts (17 and  $29\text{ MWm}^{-1}$  are defined for EU and JA DEMO concepts, respectively) [10]. One can also use a limit linked to the peak heat flux in the SOL when the plasma re-attaches to the divertor based on [11]. This protection constraint is defined in PROCESS by placing an upper limit on:

$$\frac{P_{sep}B_T}{qAR_0} \quad (2)$$

where  $B_T$  is the on-axis toroidal field,  $q$  is the safety factor at the 95% flux surface and  $A$  is the aspect ratio ( $1/\epsilon$ ). Typical reference limits for EU-DEMO are  $\sim 9\text{ MW.Tm}^{-1}$ . The implementation of a 1-D SOL and divertor model in PROCESS allows the code to capture the divertor conditions in more detail than using these 0-D protection constraints.

Parameter	PROCESS	SONIC	Units
Plasma temperature at target	1.5	1.5	eV
Target total power load ( $q_{  }$ )	$1.718 \times 10^6$	$1.718 \times 10^6$	W/m <sup>2</sup>
Connection length from outboard mid-plane to target	166.5	166.5	m
Plasma current	13.5	13.5	MA
Plasma major radius	8.50	8.50	m
Plasma minor radius	2.43	2.43	m
Toroidal field on axis	5.94	5.94	T
Safety factor (95%)	4.1	4.1	-
Distance of flux tube from separatrix at outboard mid-plane	0.002	N/A	m
Distance of flux tube from separatrix at target	0.022	N/A	m
Radial position of outer strike point	8.16	8.16	m
Target angle in poloidal plane	25	25	degrees
Impurity fraction in SOL (Argon only)	$6 \times 10^{-3}$	varies	-
Fraction of total separatrix power going towards outboard target	0.44	calculated	-

**Table 1:** Input parameters for the comparison between *PROCESS* and *SONIC*. Note that the temperature of the plasma at the target and the total target power load are inputs for this *PROCESS* run (even though they can be chosen as bounded free parameters).

Name	Description	Units	Name	Description	Units
$n_{01}$	Number density of slow neutral atoms	m <sup>-3</sup>	$n_{02}$	Number density of fast neutral atoms	m <sup>-3</sup>
$n_{i,e}$	Electron/ion number density ( $n = n_e = n_i$ )	m <sup>-3</sup>	$v$	Plasma flow velocity	ms <sup>-1</sup> ]
$T_{i,e}$	Electron/ion temperature	eV	$q_{  }$	Parallel SOL power density	W/m <sup>2</sup>
$m_i$	Mass of ion $i$	kg	$c_{s0}$	Ion sound speed at target	ms <sup>-1</sup>
$A_0$	Area of SOL at the target	m <sup>2</sup>	$T$	Plasma temperature at target	eV
$R_{ion}$	Rate coef. for ionisation of hydrogenic species by electron impact	s <sup>-1</sup>	$R_{rec}$	Rate coef. for volume recombination of hydrogenic species	s <sup>-1</sup>
$R_{CX}$	Rate coef. for CX of hydrogenic species	s <sup>-1</sup>	$P_{LT}$	Line radiation power rate coef.	Wm <sup>3</sup>
$P_{RB}$	Continuum radiation power rate coef.	Wm <sup>3</sup>	$\kappa_0$	Thermal conductivity parameter	Wm <sup>-1</sup> K <sup>-1</sup>

**Table 2:** Parameters of the *PROCESS* divertor model.

## 2.1 PROCESS Divertor Model

The 1-D SOL and divertor model in *PROCESS* contains a set of ordinary differential equations derived from [12] to describe the physical processes in the SOL. The geometry for the model is shown in Figure 1 in [12]. It should be noted that the calculation direction is from the target to the midplane (hence the minus sign in eqn. 3). The model assumes all particles striking the target are recycled (i.e. no pumping). The physical processes that are included in the model are given in the equations in this section (see Table 2 for parameter definitions). For more detailed discussion on the calculations see [12, 13]. The processes captured in the model are: convected heat flux (eqn. 3), parallel thermal conduction (eqn. 5), momentum conservation (eqn. 6), radiation by D, T and impurities (eqns. 7 and 8), charge exchange (eqn. 9), electron impact ionisation (eqn. 10), surface recombination (eqn. 11) and energy conservation (eqn. 12).

$$q_{||,conv} = -nv \left( 5eT + \frac{1}{2}m_i v^2 \right) \quad (3)$$

$$P_{tot} = n(m_i v^2 + 2eT) \quad (4)$$

$$\frac{dT}{dx} = q_{||cond} \frac{1}{T^{5/2} \kappa_0} \quad (5)$$

$$\frac{dP_{tot}}{dx} = -(R_{CX}(n_{01} + n_{02}) + R_{rec}n)(nv)m_i \quad (6)$$

$$\rho_H = (n_{01} + n_{02})(P_{LT} + P_{RB})n \quad (7)$$

$$\rho_{imp} = n^2 \sum_Z c_Z L_Z \quad (8)$$

$$\rho_{CX} = eT_e R_{CX} (n_{01} + n_{02})n \quad (9)$$

$$\rho_{ion} = (R_{ion}n_{01} + R_{ion}n_{02})eE_{ion} \quad (10)$$

$$p_{rec} = E_{rec} e n_e c_{s0} A_0 \quad (11)$$

$$\frac{dQ}{dx} = A(\rho_{imp} + \rho_H + \rho_{CX} + \rho_{ion}) \quad (12)$$

As there is no general expression for the thermal conductivity of a multi-species plasma, an approximation is used from [14]. The 'slow' and 'fast' neutrals have the following continuity equations.

$$\frac{dn_{01}}{dx} = \frac{1}{v_{01}}(R_{rec}n^2 - R_{ion}n_{01}n) \quad (13)$$

$$\frac{dn_{02}}{dx} = -\frac{1}{v_{02}}R_{ion}n_{02}n \quad (14)$$

The cross-section area of the SOL,  $A$ , is calculated by taking the radial width equal to the power fall-off length. Total heat flux,  $q_{||tot}$  is derived from the total power in the SOL,  $Q$ .

$$q_{||tot} = \frac{Q}{A} \quad (15)$$

The conducted heat flux is then:

$$q_{||cond} = q_{||total} - q_{||conv} \quad (16)$$

The flux tube used in the model begins at the edge of the target sheath and ends at the plasma outboard mid-plane. The PROCESS code takes a number of input parameters (see Table 1), and constraints defined by the user. Importantly, the parallel heat flux on the target  $q_{||}$  and the target temperature  $T_{target}$  are bounded free parameters. This allows the user to constrain both values to ensure plasma detachment. The model then calculates backwards from the target to the outboard mid-plane to determine what upstream parameters produce the prescribed target conditions. The radiation calculations are based on ADAS loss data for the impurity species available in PROCESS [15]. The code enforces consistency between the calculated upstream  $P_{sep}$  from the 1-D model and the  $P_{sep}$  calculated by the core physics model (alpha power minus radiation losses).

## 2.2 SONIC Simulation

The SONIC modelling software is a 2-D divertor and SOL simulation suite that consists of a number of codes that model different physical aspects of the divertor and SOL. SONIC consists of three transport codes:

- IMPMC – a 2-D Monte Carlo impurity code
- SOLDOR – a 2-D plasma fluid code for ion and electron components
- NEUT2D – a 2-D Monte Carlo neutral transport code

The code calculates the properties of the divertor and SOL plasmas for a 2-D geometry and therefore it calculates over multiple flux tubes, from the separatrix to  $\sim 3$  cm outer SOL. Radial transport coefficients are taken from ITER simulations ( $\chi_i = \chi_e = 1\text{m}^2\text{s}^{-1}$ ,  $D = 0.3$ ) [16–18]. The drift transport across the flux tubes is not included in SONIC. For comparison of local quantities, a single flux tube was identified that is the same radial distance from the separatrix at the outboard mid-plane as used in the PROCESS model (2mm). The integrated quantities for the comparison, such as the total impurity radiation power in the outer divertor SOL, use quantities from SONIC that include all

of the outer divertor flux tubes. As SONIC captures the physics process across multiple flux tubes it can simulate the radial distribution of the detachment, i.e. “full” or “partial”, unlike the 1-D model.

In the Japanese DEMO case used in the comparison [6], the plasma is attached radially away from the strike point along the target ( $> 12$  cm), and the electron temperature at the target increases radially from 1-2 eV in the detached area to 20-30 eV in the attached area. The peak heat load appears in the attached area. For the purpose of power handling, this comparison will show appearance of the detachment near the strike point, as most of the power is transported near the separatrix, where the power fall-off in DEMO size machines is of the order 2mm [11].

## 2.3 Inputs

The single flux tube modelled in PROCESS (2 mm from the separatrix at the mid-plane) was compared to information on the corresponding flux tube extracted from the SONIC output for a Japanese DEMO design [6]. The input data for PROCESS is listed in Table 1.

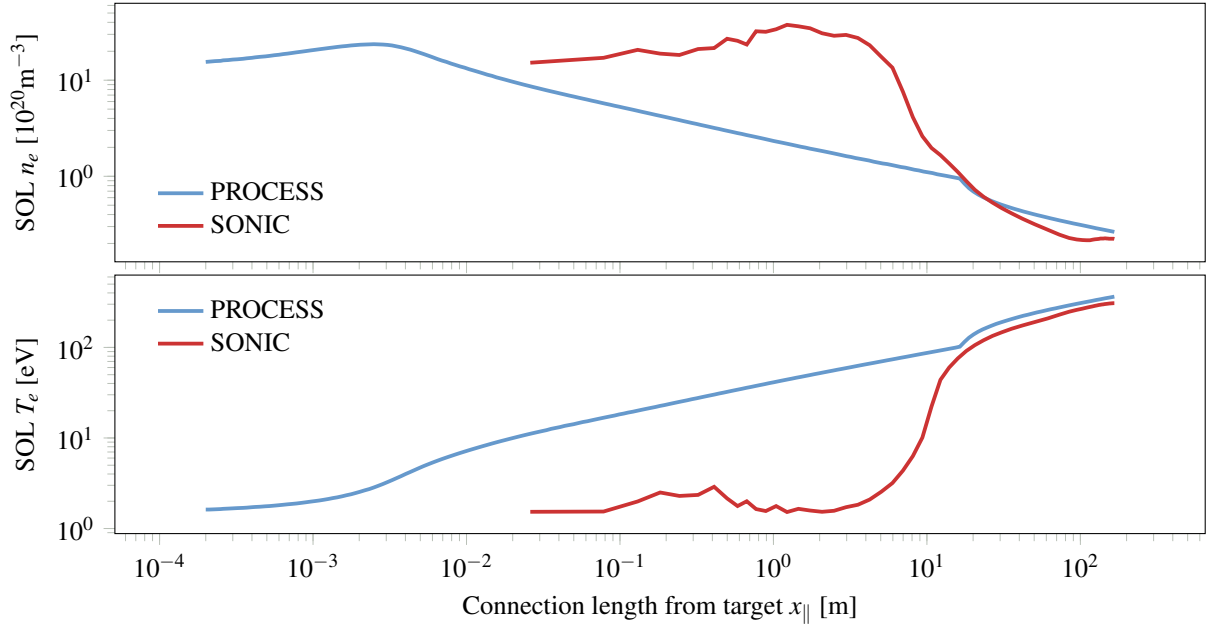
## 3 Results

Figure 1 shows the plasma temperature ( $T_e$ ) and density ( $n_e$ ) along the flux tube, where left and right ends correspond to the target and outboard mid-plane, respectively. Values of  $T_e$  and  $n_e$  calculated by PROCESS and SONIC are similar at the both ends. The two profiles from PROCESS and SONIC show similar values upstream of the X-point, and different behavior below the X-point. This is due to the fact that SONIC includes physical processes that are not incorporated in the system code; SONIC simulates impurity transport along the flux tube as well as diffusion process, whereas PROCESS uses a fixed value of the impurity fraction (see Figure 2).

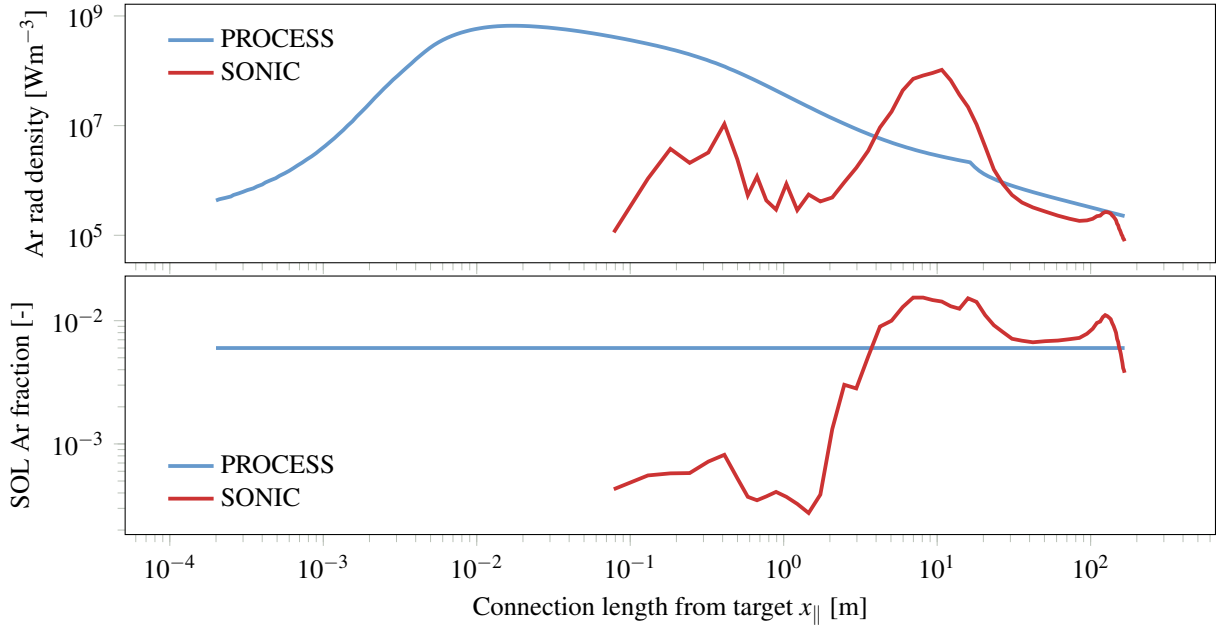
It is noted that SONIC simulations are still not consistent with experimental results. Improvement of the plasma detachment modelling will be necessary. The 1-D model allows multiple impurities (e.g. xenon in the plasma core and argon and small amounts of tungsten in the SOL). For this comparison only argon in the SOL is considered. In reality there will be a mixture of elements present in the core and SOL depending on the seeded impurity choice and first wall/divertor material choice.

Figure 2 shows profiles of the argon impurity radiation power density and the impurity fraction along the flux tube. Note for SONIC that values of impurity parameters at the sheath entrance are not shown. For the SONIC results, the Ar radiation power density is significantly increased at approximately the midpoint between the x-point and divertor target due to an increase in both  $n_e$  and the Ar fraction.  $T_e$  is reduced to the detached plasma level, i.e. 1-2 eV, downstream of the peak. In the PROCESS model,  $T_e$  decreases monotonically from the X-point to the target. Argon radiation power density peaks just above the target.

The total impurity radiation integrated along the flux tube for the outer divertor is in reasonable agreement, provided that we



**Figure 1:** Top: SOL plasma electron density along the connection length (target=0m, outboard mid-plane=166m) for PROCESS and SONIC. Bottom: SOL plasma temperature as a fraction of the electron density along the connection length.



**Figure 2:** Top: SOL argon impurity radiation density along the connection length (target=0m, outboard mid-plane=166m) for PROCESS and SONIC. Bottom: SOL argon impurity as a fraction of the electron density along the connection length.

give an value of the impurity concentration comparable to that in the core plasma, i.e. 0.6% (see Table 3). It is worth noting that the SONIC profile in Figures 1 and 2 shows a single flux tube, but the total radiation power from SONIC is over all of the flux tubes. PROCESS uses the single flux tube to provide results for the entire outer divertor.

The calculated power crossing the separatrix  $P_{sep}$  is in reasonable agreement as well as the plasma parameters such as

$n_e$  and  $T_e$  at the target and mid-plane, once we give an reasonable value of the impurity concentration, even though the profiles in the SOL are not accurately simulated by the 1-D code.

Figure 3 shows scans of  $P_{sep}$  in PROCESS for a DEMO-like machine plotted against the machine major radius,  $R_0$ . It shows that inside PROCESS the major radius is more dependent on  $P_{sep}$  at  $P_{sep} > 200$  MW. The values of  $P_{sep}$  found in JA-DEMO are in the region where it more strongly influences the size. However,

Parameter	PROCESS	SONIC	Units
Total power conducted across the plasma separatrix	241	258	MW
SOL electron density at outboard target	155	152	$10^{19}\text{m}^{-3}$
SOL electron temperature at outboard mid-plane	364	308	eV
SOL electron density at outboard mid-plane	2.64	2.23	$10^{19}\text{m}^{-3}$
Total Argon impurity radiation (outer divertor SOL)	72.6	79	MW

**Table 3:** Table of PROCESS and SONIC output parameters for the comparison.

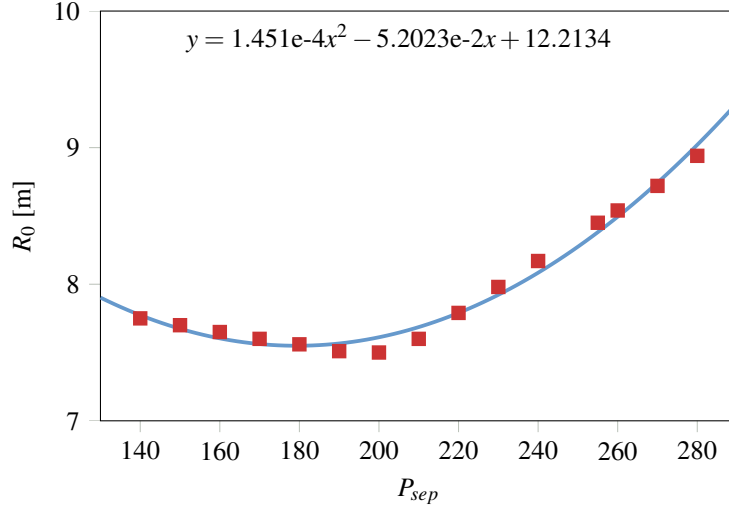


**Figure 3:** Machine major radius versus  $P_{sep}$  for a number of PROCESS runs scanning the minimum allowable  $P_{sep}$ . Red squares are individual PROCESS runs and the blue line is a polynomial fit.

EU-DEMO with  $P_{sep} \sim 150$  MW sits in the region where the size appears to have little dependence on  $P_{sep}$ . The major radius is closely linked with the overall cost of the machine and serves as a useful proxy. As the PROCESS model has only been compared to one JA-DEMO case it is not yet clear how large the differences are for a more general case. Additionally the value of  $P_{sep}$  is only one of the outputs from the model, the accuracy of the determination of detachment is not currently known outside of the JA-DEMO case.

## 4 Conclusions

A one dimensional divertor model in PROCESS was compared to results of SONIC simulation in conditions of partial detachment. Comparison of the plasma parameters along the flux tube near the separatrix showed agreement on the total power crossing the separatrix and rough agreement on the upstream mid-plane values of the SOL density and temperature, provided that we gave an value of the impurity concentration comparable to that in the core plasma.

Good agreement of the total outer divertor impurity radiation power was also seen. However, differences of the plasma and impurity profiles were seen along the divertor leg, since the SONIC code simulated numbers of physical processes not

accounted for in simple 1-D model with a fixed value of the impurity fraction. User inputs are used to constrain the boundary conditions such as the target SOL temperature and the allowable maximum heat load on the target. As a result, we found that the simple divertor model in PROCESS will predict a formation of the divertor detachment simulated by 2-D divertor code.

The impact of the uncertainty on  $P_{sep}$  has been investigated for a DEMO-like machine and the dependence of size and cost and  $P_{sep}$  shows a relatively flat region up to  $\sim 200$  MW. This would indicate that for use of the model for EU-DEMO the impact of the 5-10% difference in the comparison will have a low impact of the machine size and cost; two key design parameters.

A larger sample of 2-D simulations would be ideal for future comparisons with the 1-D model. A comparison of the 1-D model to the European 2-D SOL and divertor modelling code SOLPS [19] for EU-DEMO would also be beneficial and is currently planned.

## Acknowledgements

This work was funded by the RCUK Energy Programme [grant number EP/T012250/1]. This work has been carried out within the framework of the EUROfusion Consortium and has received funding from the Euratom research and training programme

2014-2018 and 2019-2020 under grant agreement No 633053. The views and opinions expressed herein do not necessarily reflect those of the European Commission.

This work was carried out within the framework of the Broader Approach DEMO Design Activity (DDA). Contributions by all members of JA and EU Home Teams for BA DDA are greatly appreciated. This work was also supported by the Joint Special Design Team for Fusion DEMO in Japan.

This work was carried out using the JFRS-1 supercomputer system at Computational Simulation Centre of International Fusion Energy Research Centre (IFERC-CSC) in Rokkasho Fusion Institute of QST (Aomori, Japan).

## References

- [1] G. Federici, *et al.*, “DEMO design activity in Europe: Progress and updates,” *Fusion Engineering and Design*, vol. 136, pp. 729–741, jun 2018.
- [2] EUROfusion, “European Research Roadmap to the Realisation of Fusion Energy,” <https://www.euro-fusion.org/eurofusion/roadmap/>, 2018.
- [3] M. Kovari, *et al.*, ““PROCESS”: A systems code for fusion power plants-Part 1: Physics,” *Fusion Engineering and Design*, vol. 89, pp. 3054–3069, dec 2014.
- [4] M. Kovari, *et al.*, ““PROCESS”: A systems code for fusion power plants - Part 2: Engineering,” *Fusion Engineering and Design*, vol. 104, pp. 9–20, mar 2016.
- [5] K. Shimizu, *et al.*, “Kinetic modelling of impurity transport in detached plasma for integrated divertor simulation with SONIC (SOLDOR/NEUT2D/IMP/EDDY),” *Nuclear Fusion*, vol. 49, p. 065028, jun 2009.
- [6] N. Asakura, *et al.*, “Studies of power exhaust and divertor design for a 1.5 GW-level fusion power DEMO,” *Nuclear Fusion*, vol. 57, p. 126050, dec 2017.
- [7] K. Hoshino, *et al.*, “Improvement of the detachment modelling in the SONIC simulation,” in *Journal of Nuclear Materials*, vol. 415, pp. S549–S552, North-Holland, aug 2011.
- [8] A. Kallenbach, *et al.*, “Optimized tokamak power exhaust with double radiative feedback in ASDEX Upgrade,” *Nuclear Fusion*, vol. 52, p. 122003, dec 2012.
- [9] R. P. Wenninger, *et al.*, “DEMO divertor limitations during and in between ELMS,” *Nuclear Fusion*, vol. 54, p. 114003, nov 2014.
- [10] N. Asakura, *et al.*, “Plasma exhaust and divertor studies in Japan and Europe broader approach, DEMO design activity,” *Fusion Engineering and Design*, vol. 136, pp. 1214–1220, nov 2018.
- [11] T. Eich, *et al.*, “Inter-ELM power decay length for JET and ASDEX Upgrade: Measurement and comparison with heuristic drift-based model,” *Physical Review Letters*, vol. 107, p. 215001, nov 2011.
- [12] A. Kallenbach, *et al.*, “Analytical calculations for impurity seeded partially detached divertor conditions,” *Plasma Physics and Controlled Fusion*, vol. 58, p. 045013, apr 2016.
- [13] M. Kovari, “A one-dimensional scrape-off layer model in the reactor systems code.” In preparation.
- [14] A. Huber and A. V. Chankin, “Scaling for the SOL/separatrix  $\chi_{\perp}$  following from the heuristic drift model for the power scrape-off layer width,” *Plasma Physics and Controlled Fusion*, vol. 59, p. 064007, jun 2017.
- [15] H. Lux, R. Kemp, D. J. Ward, and M. Sertoli, “Impurity radiation in DEMO systems modelling,” *Fusion Engineering and Design*, vol. 101, pp. 42–51, dec 2015.
- [16] A. S. Kukushkin, *et al.*, “2D modelling of the edge plasma in ITER,” *Contributions to Plasma Physics*, vol. 38, pp. 20–25, jan 1998.
- [17] R. Stambaugh, *et al.*, “Power and particle control,” *Nuclear Fusion*, vol. 39, pp. 2391–2369, dec 1999.
- [18] D. P. Coster, *et al.*, “SOLPS modelling of W arising from repetitive mitigated ELMS in ITER,” *Journal of Nuclear Materials*, vol. 463, pp. 620–623, aug 2015.
- [19] S. Wiesen, *et al.*, “The new SOLPS-ITER code package,” *Journal of Nuclear Materials*, vol. 463, pp. 480–484, aug 2015.